Experimental Eye Research 235 (2023) 109614

Contents lists available at ScienceDirect

Experimental Eye Research

journal homepage: www.elsevier.com/locate/yexer

Research article

Purinergic 2X 4 (P2X4), but not P2X7, receptors increase cytosolic [Ca^{2+}] and stimulate mucin secretion in rat conjunctival goblet cells to maintain ocular surface health

Haakon K. Fjærvoll [a,b,*], Ketil A. Fjærvoll [a,b], Menglu Yang [a], Jeffrey Bair [a], Tor P. Utheim [b,c,d], Darlene A. Dartt [a]

[a] Schepens Eye Research Institute, Massachusetts Eye and Ear Infirmary, Department of Ophthalmology, Harvard Medical School, Boston, MA, United States
[b] Medical Student Research Program, Institute of Clinical Medicine, Faculty of Medicine, University of Oslo, Oslo, Norway
[c] Department of Medical Biochemistry, Oslo University Hospital, Oslo, Norway
[d] Department of Oral Biology, Faculty of Dentistry, University of Oslo, Oslo, Norway

ARTICLE INFO

Keywords:
ATP
Calcium
Conjunctiva
Goblet cells
Inflammation
Ocular surface
Pannexins
Purinergic receptors

ABSTRACT

Ionotropic purinergic receptors (P2XRs) are activated by ATP and ATP analogs. ATP can be released through ATP-permeable channels such as the pannexin hemichannels. Upon activation, the P2XRs become permeable to Ca^{2+}, a potent stimulator of mucin secretion in conjunctival goblet cells (CGCs). The purpose of this study was to investigate the presence and function of P2XRs in CGCs. We also examined the presence of pannexin hemichannels. Rat first passage CGCs were stained with the goblet cell marker anti-cytokeratin 7 antibody and specific antibodies to P2X1-7 receptors and pannexin 1-3. mRNA expression was determined by RT-PCR using primers specific to P2XRs and pannexins. Proteins were identified with Western blotting (WB) using the same antibodies as for immunofluorescence (IF) microscopy. To study receptor function, CGCs were incubated with Fura 2-AM, exposed to agonists and antagonists, and intracellular [Ca^{2+}] ([Ca^{2+}]$_i$) measured. [Ca^{2+}]$_i$ was also measured after knock down of P2X4 and P2X7 receptor expression, and when exploiting P2XR specific characteristics. Lastly, mucin secretion was measured after the addition of several P2XR agonists. All P2XRs and pannexins were visualized with IF microscopy, and identified with RT-PCR and WB. [Ca^{2+}]$_i$ was significantly increased when stimulated with ATP (10^{-7}-10^{-4} M). Suramin, a non-selective P2XR antagonist at 10^{-4} M did not reduce ATP-induced peak [Ca^{2+}]$_i$. The potent P2X7 agonist, BzATP (10^{-7}-10^{-4} M) increased the [Ca^{2+}]$_i$, although to a lesser extent than ATP. When measuring [Ca^{2+}]$_i$ the effect of repeated applications of ATP at 10^{-5} or 10^{-6} M the response "desensitized" after 30–60 s. The P2X4 specific antagonist 5-BDBD decreased the P2X4 agonist, 2MeSATP,-induced [Ca^{2+}]$_i$ increase. Furthermore, siRNA against the P2X4R, but not the P2X7R, decreased agonist-induced peak [Ca^{2+}]$_i$. ATP (10^{-5} M), BzATP (10^{-4} M) and 2MeSATP (10^{-5} M) induced mucin secretion. We conclude that all seven P2XRs are present in cultured rat CGCs. Of the P2XRs, only activation of the homotrimeric P2X4R appears to increase [Ca^{2+}]$_i$ and induce mucin secretion. The P2X4R in CGCs offers a new therapeutic target for protective mucin secretion.

1. Introduction

The tear film, together with the conjunctiva and cornea, make up the ocular surface. Since these epithelial structures are constantly exposed to the external environment, they function as an important first line defense against potentially harmful chemical, physical and biological agents. The tear film can be divided into three layers. The outer lipid portion is produced by the meibomian glands (Bron et al., 2004). The middle aqueous layer is secreted mainly by the lacrimal gland and consists of water, electrolytes and antimicrobial proteins and peptides (Willcox et al., 2017; Dartt and Willcox, 2013). The innermost mucous layer consists of water, electrolytes, and soluble and membrane-spanning mucins produced by conjunctival goblet cells (CGCs) and conjunctival and corneal stratified squamous epithelial cells. The mucous layer protects the ocular surface by providing hydration and lubrication, anti-adhesive properties during the blink, and also prevents

* Corresponding author. Institute of Clinical Medicine, University of Oslo, Problemveien 11, 0313, Oslo, Norway. Tel.: +47 954 40 643.
E-mail address: haakonfj@hotmail.com (H.K. Fjærvoll).

https://doi.org/10.1016/j.exer.2023.109614
Received 7 May 2023; Received in revised form 14 July 2023; Accepted 11 August 2023
Available online 12 August 2023

pathogens from binding to the ocular surface (Gipson and Argüeso, 2003; The definition and classification of, 2007).

The conjunctiva surrounds the cornea and lines the inner eyelids and contains two major cell types (Hodges and Dartt, 2013). One cell type, the CGCs are responsible for secreting high molecular weight MUC5AC; a large, gel forming mucin integral to the mucous layer of the tear film. Depletion of the MUC5AC-producing goblet cells results in damage to the ocular surface. Mucin secretion into the tear film from CGCs is regulated by a neural reflex via parasympathetic nerves. Additionally, mucin secretion can be stimulated by inflammatory mediators increased in allergic conjunctivitis, bacterial conjunctivitis and dry eye disease (Dartt and Masli, 2014).

Although extracellular ATP is kept at low levels under normal circumstances, it can rise in both physiological and pathological conditions. ATP can be elevated in response to shear stress or strain, as well as be released by peripheral nerves along with neurotransmitters (Lohman et al., 2012; Burnstock et al., 2012). ATP levels can also rise under conditions such as hypoxia, inflammation, mechanical and osmotic stress as well as cellular damage. Pannexins release ATP in a subset of tissues during inflammation (Yang et al., 2020a; Buvinic et al., 2009; Diezmos et al., 2016). Together with purinergic type 2 (P2) X 7 receptors (R), pannexins can contribute to damage and cell death (Bernier et al., 2012; Diezmos et al., 2018). Both stress and cellular damage occur in eyes of patients with dry eye disease, and these patients have a several fold increase of ATP concentration in tears (The definition and classification of, 2007; Guzman-Aranguez et al., 2017).

The released extracellular ATP can activate membrane localized P2Rs. There are two groups of P2Rs, P2XRs and P2YRs. P2YRs are 7-transmembrane, G protein-coupled receptors that when stimulated can increase intracellular Ca^{2+} concentration ($[Ca^{2+}]_i$). The increase in $[Ca^{2+}]_i$ can then lead to multiple types of intracellular processes including mucin secretion from goblet cells (Lazarowski and Boucher, 2009). P2Y receptors are present in rat CGCs and play a role in GC function (unpublished data, 2023). In contrast to P2YRs, P2XRs are ATP-gated nonselective cation channels formed from three subunits that when activated increase the cellular permeability to Ca^{2+}, Na^{+}, and K^{+}. There are seven different P2X subunits, P2X1 through P2X7, that can form homotrimeric (all except for P2X6) or heterotrimeric (all but P2X7) receptors (Nicke et al., 2022; Torres et al., 1999). There are multiple receptor-specific features that can be used to distinguish between the P2XRs (Syed and Kennedy, 2012; Illes et al., 2021). For example, the response of P2X2 receptors is modulated in the presence of low pH, whereas all P2XRs except the P2X7 receptor desensitize by timed, repeated application of ATP (Nicke et al., 2022; Clyne et al., 2002). To date, there are agonists and antagonists specific to multiple P2XRs (Syed and Kennedy, 2012; Illes et al., 2021). P2XRs are thus potential regulators of mucin secretion. Herein, the experiments will focus on the P2X family of P2 receptors.

There is limited, published research on P2XRs in conjunctival tissue and even less on the goblet cells. P2X4R and P2X7R were identified in cultured rat and human CGCs, but these were the only subtypes investigated (McGilligan et al., 2013). Therefore, the purpose of this study was to investigate whether the other P2XRs and pannexin hemichannels are present in CGCs, and if the P2XRs function to increase $[Ca^{2+}]_i$ and secrete mucins.

2. Materials and methods

2.1. Animals

All experiments in this in vitro study were approved by the Schepens Eye Research Institute Animal Care and Use Committee and adhere to the ARVO Statement for the Use of Animals in Ophthalmic and Vision Research. Male Sprague Dawley rats weighing between 125 and 150 g obtained from Taconic Farms (Germantown, NY) were euthanized with CO_2 for 5 min and decapitated. The bulbar and forniceal conjunctiva were removed from both eyes.

2.2. Cell culture

Goblet cells were cultured from rat conjunctival explants as described previously (Shatos et al., 2003; Yang et al., 2020b). Pieces of conjunctival epithelium were placed in 6-well plates and covered with RPMI 1640 medium supplemented with 10% fetal bovine serum, 2 mM glutamine, and 100 mg/ml penicillin-streptomycin for 7–9 days. First passage goblet cells were used in all experiments. The identity of cultured goblet cells was periodically checked by evaluating fluorescence microscopy staining with the lectin Ulex europaeus agglutinin (UEA)-1 which binds to goblet cell secretory product (Shatos et al., 2003).

2.3. Reverse transcription polymerase chain reaction (RT-PCR)

RT-PCR was performed as previously reported, with minor modifications (Yang et al., 2020b). Total RNA was extracted from cultured goblet cells and purified according to the quick-start protocol for miRNeasy mini kit (Qiagen, CA). To remove any remaining DNA, total RNA lysate was treated with the TURBO DNA-free kit according to the manufacturer's instructions (Thermo Fisher, Waltham, MA). NanoDrop 2000 spectrophotometer (Thermo Scientific, Waltham, MA) was used to check total RNA concentration. Five μg of purified total RNA was used for complementary DNA (cDNA) synthesis using the Superscript III First-strand synthesis system (Invitrogen, Carlsbad, CA). The cDNA was amplified by PCR using primers specific to rat P2X1-7 and Panx1-3 with the Jumpstart REDTaq Readymix Reaction Mix (Sigma-Aldrich, St. Louis, MO) in a thermal cycler (Master Cycler, Eppendorf, Hauppauge, NY). PCR was initiated at 95 °C for 7 min and completed with a final extension for 5 min at 72 °C. The PCR program consisted of 40 cycles with the following settings: denaturation at 94 °C for 30 s, annealing at 60 °C for 30 s and extension at 72 °C for 1 min. Samples without cDNA served as negative controls. The PCR products were then separated by electrophoresis on a 1% agarose gel and visualized by GelRed (Biotium) staining. Sequences for RT-PCR were found in multiple articles (Belleannée et al., 2010; Prasad et al., 2001; Seol et al., 2011; Lai et al., 2007) and is presented in Supplemental Table 1. All primer sequences were confirmed using NCBI's Primer BLAST (https://www.ncbi.nlm.nih.gov/tools/primer-blast/).

2.4. Western blotting (WB) analysis

The WB procedures were performed as described previously with minor modifications (Yang et al., 2020b; Hodges et al., 2011). Rat CGCs were lysed in radio-immunoprecipitation assay (RIPA) buffer (10 mM Tris-HCl [pH 7.4], 150 mM NaCl, 1% deoxycholic acid, 1% Triton X-100, 0.1% sodium dodecyl sulfate, and 1 mM EDTA) in the presence of a protease inhibitor cocktail (Sigma-Aldrich, St. Louis, MO). The homogenate was centrifuged at 2000 g for 30 min at 4 °C. Proteins were separated by sodium dodecyl sulfate-polyacrylamide gel electrophoresis (SDS-PAGE) on a 12% gel and were transferred onto nitrocellulose membranes. The nitrocellulose membranes were blocked overnight at 4 °C in 5% nonfat dried milk in buffer containing 10 mM Tris-HCl (pH 8.0), 150 mM NaCl, and 0.05% Tween-20. Membranes were then incubated with primary antibodies targeting P2X1-7R or Panx1-3 at 1:200 dilution for 72 h at 4 °C followed by incubation with goat anti-rabbit IRDye 680RD (1:15000) (Li-COR) for 1 h at room temperature. β-actin detection was used as a loading control. Immunoreactive bands were visualized with the Odyssey classic imaging system (Li-COR).

2.5. Immunofluorescence (IF) microscopy

Immunofluorescence microscopy was performed as previously

described, with minor modifications (Yang et al., 2020b). First passage CGCs were cultured on coverslips and fixed with 4% paraformaldehyde. The coverslips were blocked in 1% bovine serum albumin (BSA) with 0.2% Triton X-100 in phosphate-buffered saline (PBS) for 45 min. Cells were incubated with polyclonal rabbit anti-P2X1-7R antibodies (Catalog numbers APR-022, APR-025, APR-026, APR-024, APR-027, APR-028 and APR-004) or rabbit anti-Panx1-3 antibodies (Catalog numbers ACC-233, ACC-232 and ACC-234) (Alomone Labs, Jerusalem, Israel), with the goblet cell specific anti-cytokeratin 7 (CK7) antibody (Santa Cruz Biotechnology, CA, USA), at a 1:100 dilution overnight at 4 °C. Secondary antibodies conjugated either to Cy2 (1:100) or Cy3 (1:150) (Jackson ImmunoResearch Laboratories, West Grove, PA) were incubated for 1.5 h at room temperature. Incubation with blocking peptides of P2X1-7R or Panx1-3 (Alomone Labs, Jerusalem, Israel) and with no primary antibody were used as negative controls.

2.6. Depletion of select P2XR using short interfering RNA (siRNA)

The depletion procedure was performed as previously described (Yang et al., 2020b; Li et al., 2012). Pre-designed siRNA specific to the P2X4R or P2X7R or scrambled siRNA (ssRNA) (Dharmacon, Lafayette, CO) was added at a final concentration of 100 nM in antibiotic-free RPMI 1640 medium. The media was removed after 18 h and replaced with fresh, complete RPMI 1640 medium and incubated for 48 h. To confirm the depletion of receptors from the CGCs, one well per condition was scraped, and WB analysis using antibodies against the proteins was performed as described above. The films were analyzed with Image J software (U.S. National Institute of Health, Bethesda, MD; http://imagej.nih.gov; http://rsbweb.nih.gov/ij/).

2.7. Measurement of $[Ca^{2+}]_i$

Measurement of $[Ca^{2+}]_i$ was conducted as previously reported (Yang et al., 2020b). First passage CGCs were cultured on 35-mm glass bottom culture dishes and incubated at 37 °C overnight. Cells were then incubated for 1 h in the dark at room temperature with KRB-HEPES supplemented with 0.5% BSA, 0.5 μM fura-2/AM (Invitrogen, Grand Island, NY, USA), 8 μM pluronic acid F127 (Sigma-Aldrich, St. Louis, MO, USA) and 250 μM sulfinpyrazone (Sigma-Aldrich). Prior to Ca^{2+} measurements, cells were washed with KRB-HEPES containing 250 μM sulfinpyrazone. Calcium measurements were conducted using a fluorescent ratio imaging system (In Cyt Im2; Intracellular Imaging, Cincinnati, OH, USA) with excitation wavelengths of 340 and 380 nm. Cells were exposed to agonists and antagonists, in different buffer conditions (normal pH was 7.40 ± 0.04). The $[Ca^{2+}]_i$ over time was calculated and the change in peak $[Ca^{2+}]_i$ was calculated by subtracting the average of the basal value from the peak $[Ca^{2+}]_i$ value.

The pharmacological agonists and antagonists were chosen based on information from two independent comprehensive reviews (Syed and Kennedy, 2012; Illes et al., 2021). The P2XR agonists and antagonists ATP, BzATP, β,γ-methyleneadenosine (β,γ-MeATP), suramin, and A804598 as well as the cholinergic agonist carbachol (CCh) were purchased from Sigma-Aldrich (St. Louis, MO). The P2XR agonists and antagonists 2-Methylthio-ATP (2MeSATP), α,β-Methyleneadenosine (α,β-MeATP), and 5-BDBD were purchased from Tocris (Minneapolis, MN).

2.8. Measurement of high molecular-weight glycoprotein secretion

The measurement of secretion was performed as previously described (Yang et al., 2020b). First passage, rat CGCs were cultured in 24-well plates. The cells were serum starved for 2 h and then stimulated with agonists for 2 h in serum-free RPMI 1640 medium supplemented with 0.5% BSA. Goblet cell secretion was measured using an enzyme-linked lectin assay (ELLA) with the lectin UEA-I that detects rat conjunctival goblet cell high molecular-weight glycoproteins including MUC5AC. The media were collected and analyzed for the amount of lectin-detectable glycoproteins indicating goblet cell mucin secretion. Values of glycoprotein secretion were standardized by the amount of protein in each cell lysate and determined by using a Bio Rad Assay. Glycoprotein secretion was expressed as fold increase over basal that was set to 1.

2.9. Statistical analysis

All experiments were performed in triplicate on cells from at least three animals. Data are expressed as mean ± SEM (N = number). Data were analyzed using Student's t-test for two group comparisons, and One-way ANOVA with Dunnett correction in multiple group comparisons. $P < 0.05$ was considered statistically significant.

3. Results

3.1. All P2XRs and pannexins are present in rat CGCs

RT-PCR was performed on RNA extracted from rat CGCs using primers specific for P2X1-7 receptors and pannexin 1-3. Single bands of appropriate base pair number were detected for each P2X receptor and pannexin (Fig. 1A) (Supplemental Fig. 1).

Proteins from rat CGCs were separated by SDS-PAGE and P2X1-7 and Panx1-3 detected with WB using specific antibodies (Supplemental Fig. 2). Expected molecular weights in rat (*rattus norvegicus*) ranged from approximately 43 kDa (P2X4 and P2X6) to 68 kDa (P2X7) and 74 kDa (Panx2). The observed bands had higher molecular weights than expected (Fig. 1B). However, proteins can be post translationally modified so that higher molecular weights can be detected in some tissues (Burnstock, 2007). Fig. 1C shows bands of β-actin protein at the correct molecular weight.

IF microscopy was performed using the same antibodies as for WB in rat CGCs. Immunoreactivity was found for all P2X1-7 receptors and Panx1-3 (Fig. 2). Strong immunostaining was seen for P2X2-7 and Panx1 in the nuclei of cells. Nucleolar staining was absent for P2X3-4, P2X6, and Panx1-2, and nuclear staining was absent for P2X1 and Panx3. Perinuclear immunoreactivity was found for P2X1 and possibly P2X2. Strings of immunoreactive bands were seen for P2X2 and Panx3. Diffuse punctate cytosolic staining was detected for P2X1, P2X3-7 and Panx1-2. Apparent membrane staining was seen for P2X6 and Panx2, and possibly also P2X5 and Panx3. Peptide controls were used for each antibody indicating antibody-antigen specificity for each receptor and pannexin (Supplemental Fig. 3) and omission of primary antibody for negative controls (Supplemental Fig. 4).

3.2. P2X4 and/or P2X7Rs are functional in rat CGCs

To evaluate the effect of the non-specific P2XR agonist ATP, rat CGCs containing fura-2 were stimulated with ATP (10^{-7}-10^{-4} M) and $[Ca^{2+}]_i$ was measured. ATP significantly increased $[Ca^{2+}]_i$ in a dose-dependent manner from 66 ± 15 and 811 ± 132 nM for ATP 10^{-7} and 10^{-6} M, to 1363 ± 180 nM for ATP 10^{-5} M, before declining to 1069 ± 52 nM at ATP 10^{-4} M (N = 3) (Fig. 3A and B). These data can indicate that one or more P2X receptors are functional in rat CGCs, but other receptors, such as the P2Y class of P2 receptors can be functional as well. Study of P2Y receptors is beyond the scope of the present manuscript.

Suramin is known as a nonselective antagonist for all homotrimeric P2X receptors except for the P2X4 and P2X7 receptors. Suramin is also known to antagonize ATP at the P2X2/6, P2X2/3 and P2X4/6 heterotrimeric receptors (Syed and Kennedy, 2012; Illes et al., 2021; Burnstock, 2007). To determine which P2X receptors are functional, rat CGCs were preincubated with suramin 10^{-4} M for 10 min before stimulation with ATP 10^{-5} M. Fig. 3C shows the $[Ca^{2+}]_i$ over time. As shown in Fig. 3D, no statistically significant difference in peak $[Ca^{2+}]_i$ was seen between the two conditions. In the absence of suramin 10^{-4} M, ATP

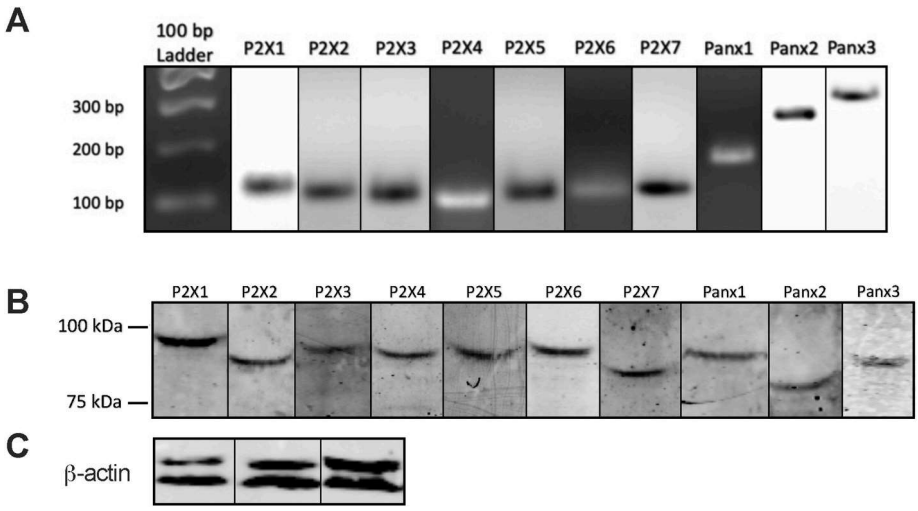

Fig. 1. Presence of P2X receptors and pannexins in rat conjunctival goblet cells. The presence of P2X1-7 receptors and pannexins were determined by RT-PCR (A) and Western blotting (B). Bands from both A and B are representative from at least three rats. β-actin protein is from each of the three rats (C). All bands are from separate gels.

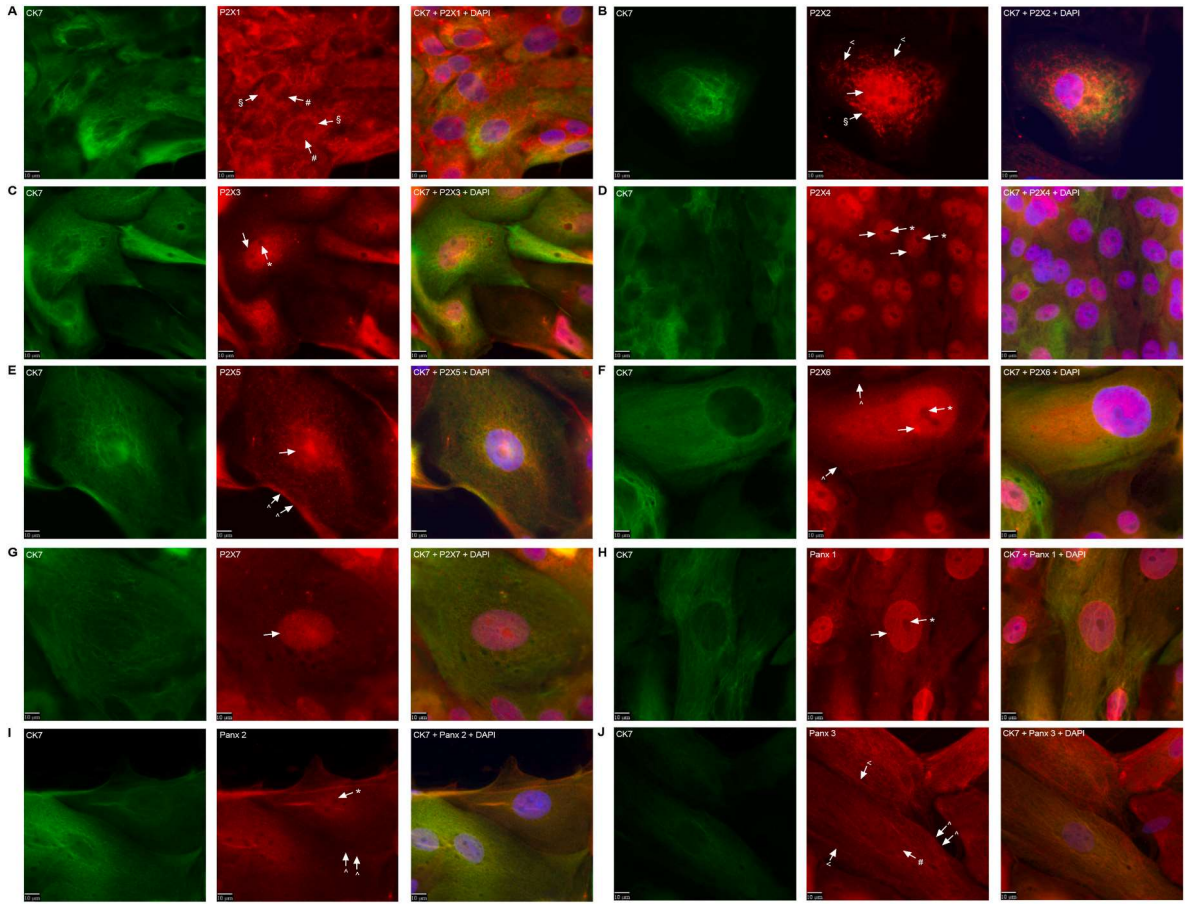

Fig. 2. Localization of P2X receptors and pannexins (Panx) in rat conjunctival goblet cells. Immunofluorescence microscopy was used to determine the localization of P2X1-7 receptors and Panx1-3. Green: Cytokeratin 7, red: P2X receptors and pannexin 1-3, blue: DAPI. Images are representative for at least four rats. Plane arrows indicate nuclei of cells. Arrows with * indicate the absence of nucleoli staining. Arrows with # indicate the absence of nuclei staining. Arrows with § indicate perinuclear staining. Arrows with < indicate strings of immunoreactivity. Arrows with ^ indicate membrane staining. Magnification, X1000. Representative of results from three different animals. (For interpretation of the references to colour in this figure legend, the reader is referred to the Web version of this article.)

10^{-5} M increased $[Ca^{2+}]_i$ to 365 ± 72 nM, while this value was 387 ± 40 nM after preincubating CGCs with suramin 10^{-4} M (N = 3). This suggests that the homomeric P2X4 and/or P2X7R are functional in rat CGCs, although an ATP concentration as high as 10^{-4} M is reported to be required for P2X7R activation (Syed and Kennedy, 2012; Illes et al., 2021).

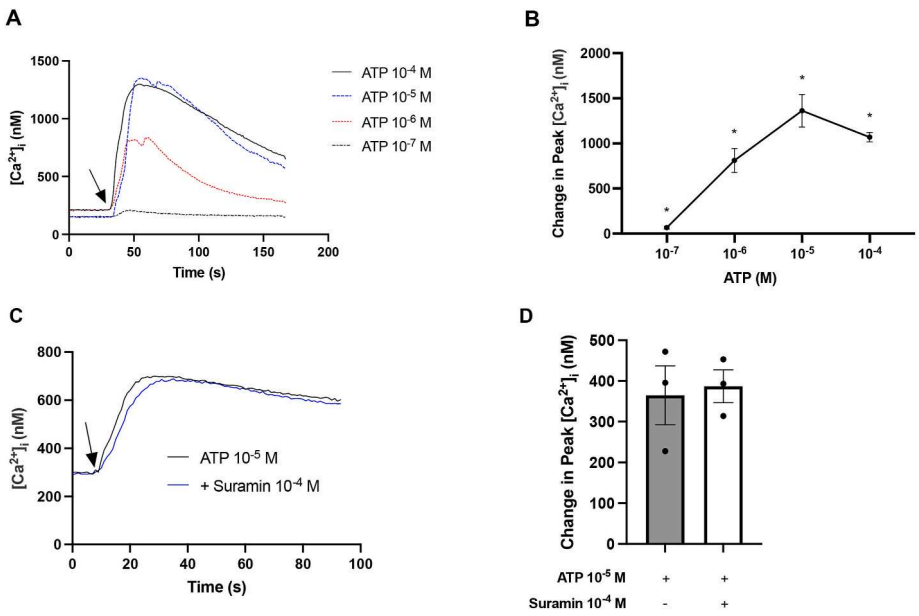

Fig. 3. Effect of ATP and suramin on $[Ca^{2+}]_i$ in rat conjunctival goblet cells (CGCs). CGCs containing fura-2 were stimulated with ATP (10^{-7}-10^{-4} M) (A and B). The average $[Ca^{2+}]_i$ level for three animals over time is shown in (A). Arrow represents the addition of ATP. (B) shows the peak increase of $[Ca^{2+}]_i$ above baseline. (C) and (D) show the effect of the nonselective P2X receptor antagonist suramin on ATP-stimulated $[Ca^{2+}]_i$. CGCs were preincubated with suramin 10^{-4} M before stimulation with ATP 10^{-5} M. (C) represents the average of three rats and shows $[Ca^{2+}]_i$ over time. Arrow represents the addition of ATP. (D) shows the peak increase of $[Ca^{2+}]_i$ above baseline. Data are shown as mean ± SEM (N = 3). * indicates significance above baseline.

Micromolar concentrations of α,β-MeATP are known to activate P2X1 and P2X3 receptors, while β,γ-MeATP only activates P2X1 at these concentrations (Illes et al., 2021). When stimulating rat CGCs with either agonist at micromolar concentrations, no significant increase in peak $[Ca^{2+}]_i$ was observed. However, both agonists gave a slight increase in peak $[Ca^{2+}]_i$ at 10^{-4} M concentration (Supplemental Fig. 5). At this concentration the two agonists can activate other P2X receptors (Syed and Kennedy, 2012; Illes et al., 2021; Palygin et al., 2018). P2X2 receptors are known to be potentiated at low pH in response to ATP stimulation (Nicke et al., 2022; Illes et al., 2021; Clyne et al., 2002). ATP-induced peak $[Ca^{2+}]_i$, however, did not significantly change when lowering the pH from 7.4 to 6.8 (Supplemental Fig. 6). Therefore consistent with the suramin experiment in Fig. 3, P2X1-3Rs are unlikely the predominant P2XRs responsible for $[Ca^{2+}]_i$ increase in rat CGCs.

Action of the P2X4R Agonist 2MeSATP on Peak $[Ca^{2+}]_i$ and the P2X4 Specific Antagonist 5-BDBD or P2X4R siRNA on 2MeSATP-induced Peak $[Ca^{2+}]_i$

Since the suramin experiment supports that the P2X4R is functional, the P2X4R agonist 2MeSATP was chosen to further evaluate the action of the P2X4 receptor (Illes et al., 2021; Zhang et al., 2007). Among available agonists, 2MeSATP has a high potency for the P2X4 receptor compared to other agonists (Illes et al., 2021; Zhang et al., 2007). Therefore, rat CGCs incubated in fura-2 AM were subjected to 2MeSATP (10^{-7}-10^{-5} M) stimulation and $[Ca^{2+}]_i$ was measured. 2MeSATP increased $[Ca^{2+}]_i$ significantly over baseline in a dose dependent manner from 64 ± 6 nM at 2MeSATP 10^{-7} M, to 91 ± 16 nM at 2MesATP 10^{-6} M and 253 ± 35 at 2MesATP 10^{-5} M (N = 3) (Fig. 4A and B).

To further demonstrate that P2X4Rs increase $[Ca^{2+}]_i$ in cultured rat CGCs, cells were incubated for 30 min in the presence of the specific P2X4R antagonist 5-BDBD (10^{-7}-10^{-5} M) and stimulated with 2MeSATP 10^{-5} M. Fig. 4C shows the $[Ca^{2+}]_i$ over time, and Fig. 4D presents the peak $[Ca^{2+}]_i$. Peak $[Ca^{2+}]_i$ significantly decreased from 243 ± 25 nM with 2MeSATP 10^{-5} M stimulation alone, to 112 ± 28 nM at 2MeSATP 10^{-5} M plus 5-BDBD 10^{-7} M (N = 3).

To confirm that the peak $[Ca^{2+}]_i$ was elicited by the P2X4 receptor, cultured rat CGCs were treated with a non-pharmacologic inhibitor 100 nM of P2X4 siRNA before stimulation with 2MesATP (10^{-6} or 10^{-5} M) and $[Ca^{2+}]_i$ was measured. The knockdown percentage of P2X4 receptor expression after siRNA and ssRNA was calculated by WB analysis (Supplemental Fig. 7), and was down by 62% and 16%, respectively, compared to non-transfected cells. As shown in Fig. 4E, peak $[Ca^{2+}]_i$ significantly decreased from 328 ± 58 and 380 ± 55 nM for non-transfected CGCs stimulated with 2MeSATP 10^{-6} and 10^{-5} M, respectively, to 140 ± 21 and 181 ± 48 nM for CGCs transfected with siRNA. ssRNA, the negative control, did not significantly alter the 2MesATP-peak $[Ca^{2+}]_i$ (N = 5).

The results from the lack of antagonism by suramin, stimulation by a P2X4R agonist, as well as a reduction by a P2X4R specific pharmacologic antagonist and P2X4R depletion by siRNA confirm that P2X4 receptors are one of the predominant P2XRs that increase $[Ca^{2+}]_i$ in rat CGCs.

Effect of Time Intervals on Sequential Additions of ATP to Increase Peak $[Ca^{2+}]_i$

P2X receptors with repeated applications of ATP desensitize at different time intervals. P2X1 and P2X3 desensitize within milliseconds, P2X4 within tens of seconds, and P2X2 and P2X5 within minutes, but the P2X7 receptor does not desensitize (Hodges et al., 2011; North, 2002). To determine which of the P2XRs that are predominantly functional in CGCs, ATP (10^{-6} or 10^{-5} M) was added four times at 30 s intervals to rat CGCs containing fura-2 while recording $[Ca^{2+}]_i$ (Fig. 5A and C). The first application of ATP at 10^{-5} M elicited a peak $[Ca^{2+}]_i$ of 392 ± 24 nM (B) (N = 3), and 305 ± 15 for ATP at 10^{-6} M (D) (N = 4). Peak $[Ca^{2+}]_i$ was significantly down by the third application for both ATP 10^{-5} and 10^{-6} M $[Ca^{2+}]_i$ was now 305 ± 16 nM at ATP 10^{-5} M (B), and 203 ± 39 at ATP 10^{-6} M (D). These data indicate that the P2X receptor of interest desensitizes within 30–60 s, and therefore the P2X4R (tens of seconds desensitization) could be responsible for some of the change in $[Ca^{2+}]_i$ seen after addition of ATP.

Action of P2X7 Agonist BzATP, Antagonist A804598 or knockdown of protein on $[Ca^{2+}]_i$

BzATP is a potent P2X7 agonist (Donnelly-Roberts et al., 2009; Brandao-Burch et al., 2012; Paredes-Gamero et al., 2004). Therefore, BzATP (10^{-7}-10^{-4} M) was added to rat CGCs containing fura-2 and $[Ca^{2+}]_i$ measured. Fig. 6A presents the average $[Ca^{2+}]_i$ over time and 6B the change in peak $[Ca^{2+}]_i$. BzATP elicited a concentration-dependent increase in $[Ca^{2+}]_i$ from 49 ± 11 nM at 10^{-7} M to 53 ± 6, 198 ± 98 and 764 ± 88 nM at 10^{-6}, 10^{-5} and 10^{-4} M BzATP, respectively (Fig. 6B) (N = 3).

To determine if BzATP activates P2X7 receptors, rat CGCs were incubated with a pharmacological antagonist, the potent competitive P2X7 antagonist A804598 (10^{-9}-10^{-6} M) for 30 min before stimulation with BzATP 10^{-4} M and $[Ca^{2+}]_i$ measured. Fig. 6C shows the average $[Ca^{2+}]_i$ over time, while Fig. 6D shows peak $[Ca^{2+}]_i$ in response to

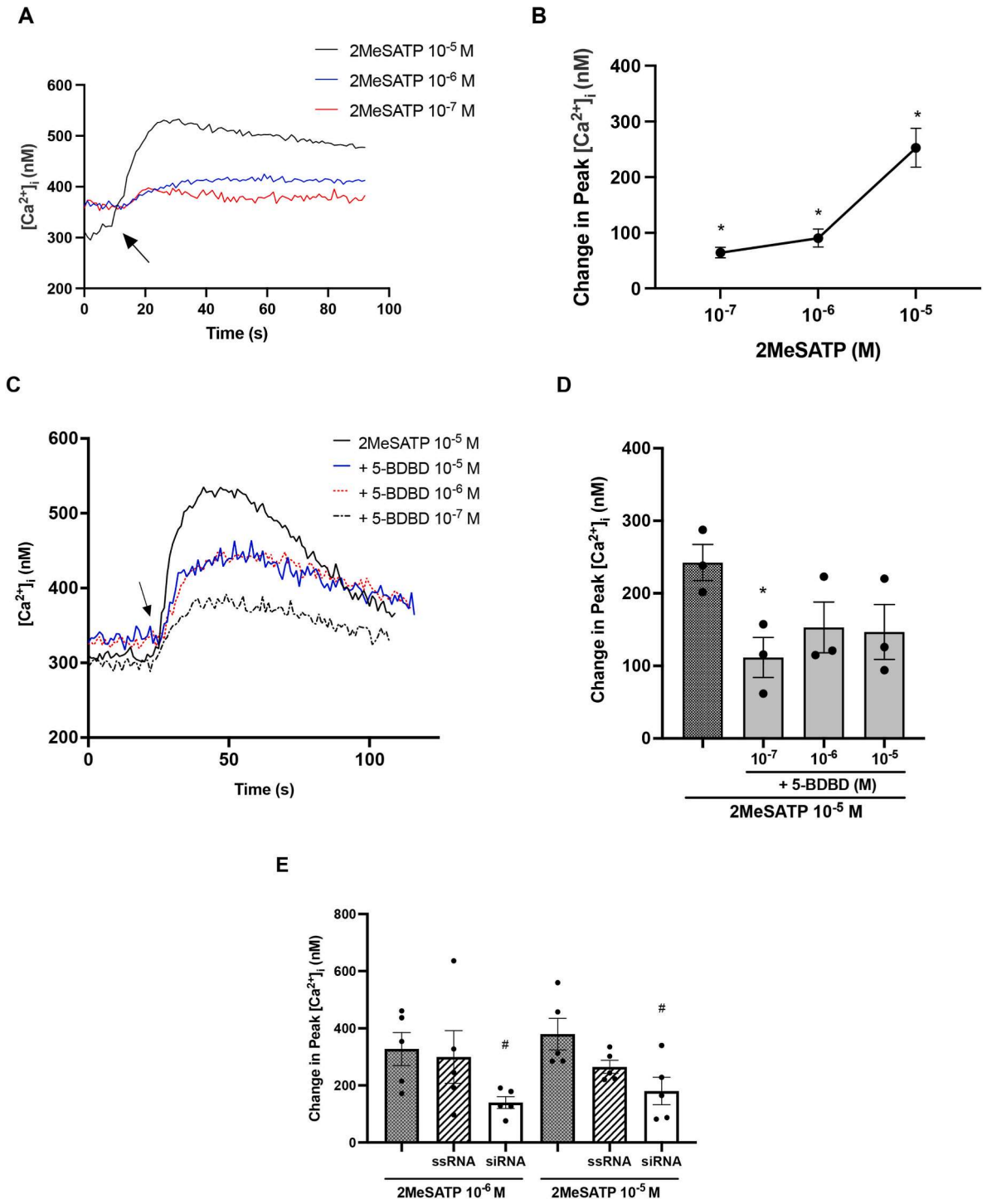

Fig. 4. Effect of P2X4R agonist, antagonist and decreased amount of P2X4R on $[Ca^{2+}]_i$. (A) and (B) show the effect of 2MesATP on $[Ca^{2+}]_i$ in cultured rat conjunctival goblet cells (CGCs). Cells were stimulated with 2MeSATP (10^{-7}-10^{-5} M). The average $[Ca^{2+}]_i$ for four animals over time is shown in (A). (B) represents the peak increase of $[Ca^{2+}]_i$ above baseline. (C) and (D) represent the effect of the P2X4 receptor antagonist 5-BDBD on 2MeSATP-stimulated peak $[Ca^{2+}]_i$. Cultured rat CGCs were preincubated with 5-BDBD (10^{-7}-10^{-5} M) for 30 min before stimulation with 2MeSATP (10^{-5} M). (C) represents the average $[Ca^{2+}]_i$ over time. Arrows represent the addition of 2MeSATP. (D) presents the peak increase of $[Ca^{2+}]_i$ above baseline. Dark grey bar represents 2MeSATP alone; light grey bars represent incubation with increasing concentrations of 5-BDBD. N = 3. * indicates significant difference from dark grey bar. (E) presents the effect of knockdown of P2X4R expression on 2MeSATP-induced $[Ca^{2+}]_i$ peak. Rat CGCs were transfected with no siRNA (dark grey bars), scrambled siRNA (ssRNA) (striped bars), or 100 nM of P2X4 siRNA (white bars) before addition of 2MeSATP (10^{-6} or 10^{-5} M). Data are presented as mean ± SEM. N = 5. # indicates significant difference from dark grey and striped bars.

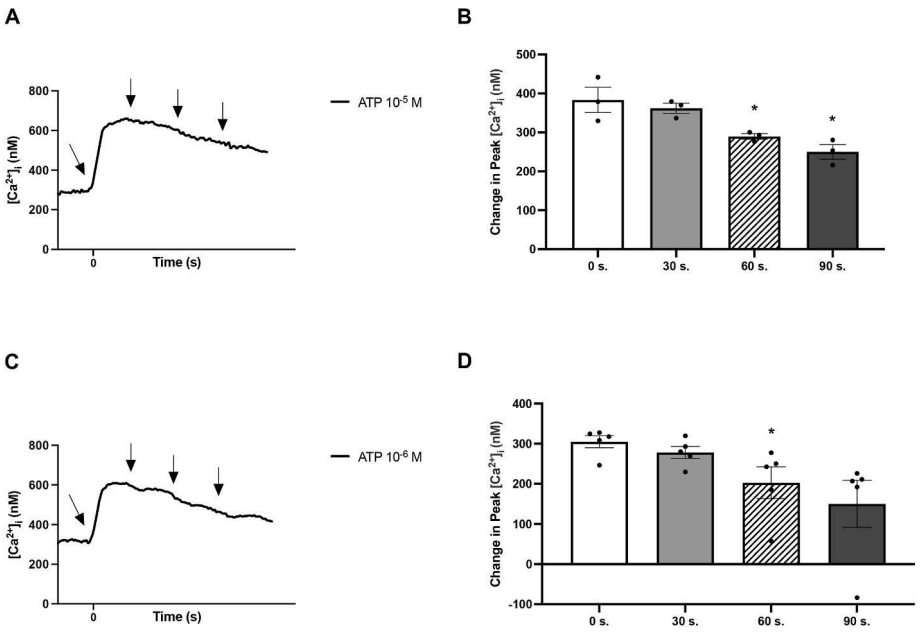

Fig. 5. Effect of repeated ATP additions on $[Ca^{2+}]_i$. ATP was added every 30 s to fura-2 containing rat conjunctival goblet cells and $[Ca^{2+}]_i$ was measured. (A) and (C) represent the average $[Ca^{2+}]_i$ over time after the addition of ATP 10^{-5} and 10^{-6} M. Arrows represent the addition of ATP. (B) and (D) show the peak increase of $[Ca^{2+}]_i$ above baseline. Data are presented as mean ± SEM. * indicates significant difference from white bars. N = 3 for (A) and (B), N = 4 for (C) and (D).

BzATP application. As presented in Fig. 6D, no significant difference in peak $[Ca^{2+}]_i$ was found between BzATP alone and with A804598. BzATP 10^{-4} M alone increased $[Ca^{2+}]_i$ to 991 ± 86 nM, while this value was 919 ± 108, 1019 ± 122, 1039 ± 118 and 1001 ± 151 nM for CGCs preincubated with 10^{-9}, 10^{-8}, 10^{-7} and 10^{-6} M of A804598, respectively (N = 3).

As a non-pharmacologic mechanism to determine if BzATP acts through the P2X7 receptor to increase $[Ca^{2+}]_i$, siRNA at 100 nM was used to knock down the expression of this receptor in cultured rat CGCs. ssRNA was used as the negative control. The knockdown percentage of P2X7 receptor expression with use of siRNA was determined by WB analysis and was down by 69%, compared to non-transfected cells. When ssRNA was used the P2X7R expression was up by 4%, compared to non-transfected cells (Supplemental Fig. 8). $[Ca^{2+}]_i$ over time for non-transfected cells and cells transfected with siRNA or ssRNA, in response to BzATP (10^{-5}-10^{-3} M) is shown in Supplemental Fig. 9. As shown in Fig. 6E, there was no significant difference in peak $[Ca^{2+}]_i$ between non-transfected cells and cells transfected with siRNA or ssRNA, in response to BzATP (10^{-5}-10^{-3} M) addition (N = 4).

As neither the potent and selective P2X7 antagonist A804598 or the specific P2X7R protein knockdown significantly reduced BzATP-induced peak $[Ca^{2+}]_i$, the P2X7R is not likely the target for BzATP-stimulated increase in $[Ca^{2+}]_i$ in rat CGCs.

3.3. *Effect of ATP, BzATP and 2MeSATP on secretion*

To investigate if ATP (non-selective P2XR agonist), BzATP (P2X7R agonist) and 2MeSATP (P2X4R agonist) stimulate secretion, cultured rat CGCs were stimulated with agonists for 2 h before measurement of high molecular-weight glycoprotein secretion. ATP (10^{-5} M), BzATP (10^{-4} M), and 2MeSATP (10^{-5} M) stimulated high molecular-weight glycoprotein secretion to 2.5 ± 0.7, 1.6 ± 0.3 and 2.8 ± 0.7-fold over basal (N = 9) (Fig. 7). The muscarinic agonist carbachol (10^{-4} M) was the positive control. These results indicate that P2X4 activation causes the same amount of secretion as ATP and that P2X4R activation induces the same magnitude of secretion as a cholinergic agonist. Although BzATP increases $[Ca^{2+}]_i$ and stimulates secretion, it is unclear which receptor it activates in CGCs.

4. Discussion

Although mRNA and protein for all P2XRs and pannexins are present in cultured rat CGCs, the P2X4R appears to be the predominant functional P2X receptor. The P2X4R agonist, 2MeSATP activates P2X4Rs and increases mucin secretion in CGCs. The homomeric P2X4 rather than the P2X1/4 or P2X4/6 heteromeric receptors is likely to be the predominant functional P2X receptor in rat CGCs as P2X1/4 and P2X4/6R are activated by α,β-MeATP and antagonized by suramin that are not an effective agonist or antagonist in the present study (Syed and Kennedy, 2012; Stokes et al., 2017). In contrast, the P2X4R agonist 2MeSATP induced a significant increase in peak $[Ca^{2+}]_i$ and secretion in the present study (Zhang et al., 2007). The 2MeSATP peak $[Ca^{2+}]_i$ response was decreased after transfection with P2X4 siRNA and after preincubating CGCs with the potent P2X4 pharmacological antagonist 5-BDBD. In addition, the time-dependence of "desensitization" of $[Ca^{2+}]_i$ of the ATP response was consistent with that of P2X4R desensitization. Finally, suramin did not decrease ATP-induced $[Ca^{2+}]_i$ peak, which is in accordance with previous research on the homomeric P2X4 receptor that suramin does not reduce the function of this receptor (Syed and Kennedy, 2012). Ivermectin, a positive allosteric modulator of P2X4 receptors, could be used in further experiments to confirm our findings (Illes et al., 2021). Chronic inflammation upregulates the P2X4R expression in airway epithelium to augment mucin secretion from MUC5AC-producing goblet cells (Winkelmann et al., 2019). In addition, the P2X4 receptor has been implicated in fusion of late endosomes and caspase 1 activation, as well as chronic neuropathic pain, allodynia, and has secretory functions in glandular tissues (Illes et al., 2021; Winkelmann et al., 2019; Kanellopoulos et al., 2021). Herein, we showed that activation of P2X4 receptors stimulates goblet cell secretory function that could contribute to tear film homeostasis and prevention of ocular surface disease. There are, however several possible explanations to why we could not observe other functional P2XRs in this study. Firstly, we only studied changes in $[Ca^{2+}]_i$ and it is possible that some of the P2XRs mainly function through fluxes of other cations than Ca^{2+}, or that the P2XRs' conductance of calcium is too small to detect with the current method (Samways et al., 2014). Secondly, our method of Ca^{2+} measurement using receptor activation and blockage, could be inappropriately designed for measuring the Ca^{2+} conductance of specific P2XRs. For instance,

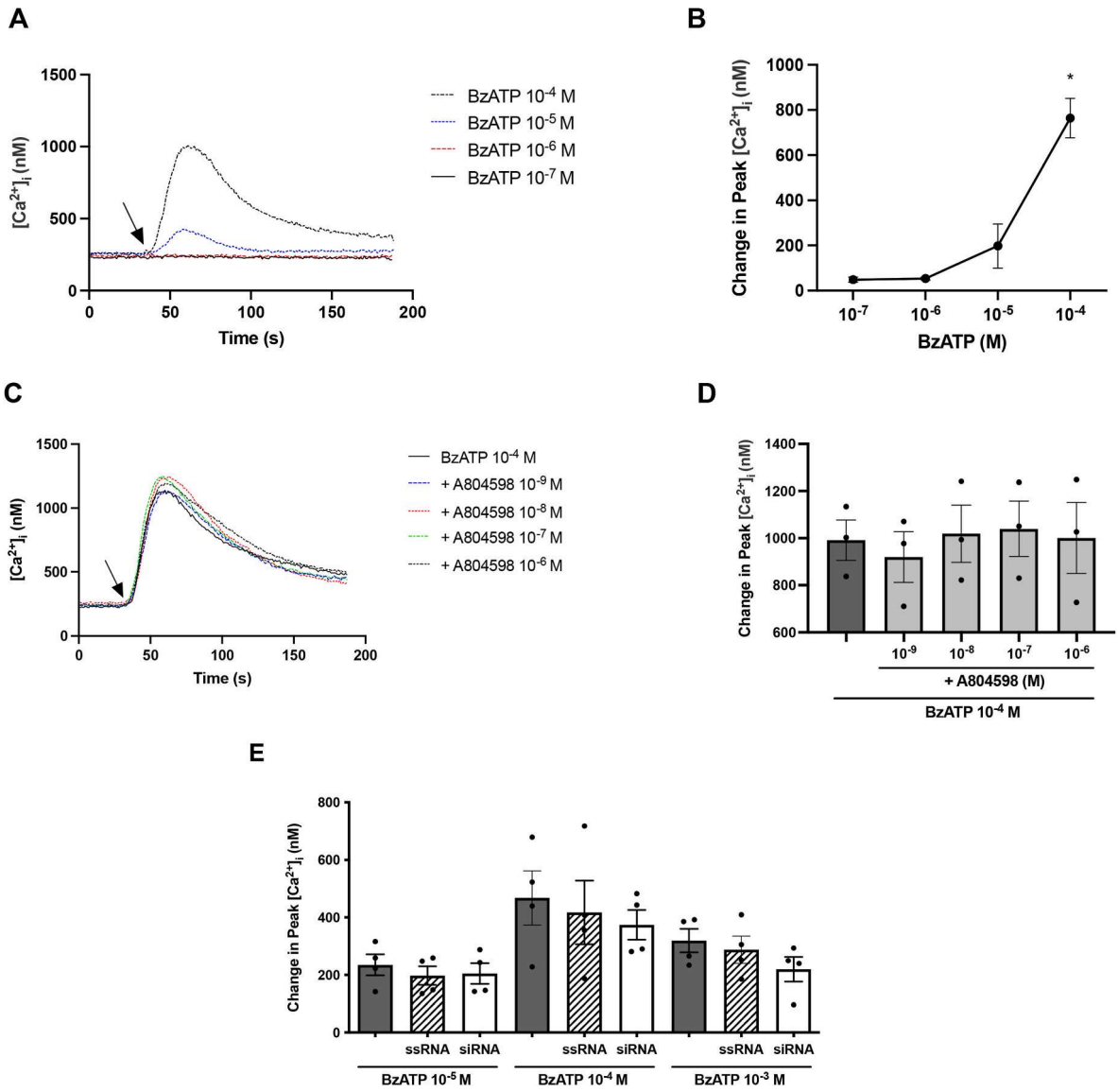

Fig. 6. Effect of P2X7R agonist, antagonist and protein expression on $[Ca^{2+}]_i$. (A) and (B) show the effect of BzATP on $[Ca^{2+}]_i$ in rat conjunctival goblet cells (CGCs). CGCs incubated with fura-2 AM were stimulated with BzATP (10^{-7}-10^{-4} M). The average $[Ca^{2+}]_i$ level in three different animals over time is shown in (A). (B) shows the peak increase of $[Ca^{2+}]_i$ above baseline for the three different animals. (C) and (D) present the effect of the potent P2X7 receptor antagonist A804598 on BzATP-stimulated peak $[Ca^{2+}]_i$. CGCs were preincubated with A804598 (10^{-9}-10^{-6} M) for 30 min before stimulation with BzATP 10^{-4} M. (C) represents the average response of three different animals and shows $[Ca^{2+}]_i$ over time. Arrows represent the addition of BzATP. (D) shows the peak increase of $[Ca^{2+}]_i$ above baseline. The dark grey bar represents BzATP alone; light grey bars represent BzATP response after incubation with A804598. N = 3. (E) represents the effect of P2X7 knockdown on BzATP-induced peak in $[Ca^{2+}]_i$. CGCs were transfected with 100 nM P2X7 siRNA, scrambled siRNA (ssRNA), or no siRNA before addition of BzATP (10^{-5}-10^{-3} M). Peak $[Ca^{2+}]_i$ was calculated for four different animals. The dark grey bar represents BzATP alone; striped bars represent BzATP response after incubation with ssRNA; white bars represent BzATP response after incubation with siRNA. All data are presented as mean ± SEM. * indicates significance above baseline.

electrophysiological experiments or knockout animals may be required to observe the actions of other P2XRs. Lastly, there may be inactive splice variants, protein complexes or post-translational modifications to some P2XRs that inhibit their function, but are still visualized with our antibodies and peptide controls.

Although P2X7Rs were detectable in CGCs by PCR, WB, and IF, we were not able to find functional P2X7Rs in rat CGCs. The potent and specific P2X7 antagonist A804598 did not decrease the BzATP-induced peak $[Ca^{2+}]_i$ or the total increase in $[Ca^{2+}]_i$ (area under curve; data not shown). Furthermore, siRNA specific to the P2X7 receptor did not decrease the BzATP-induced peak $[Ca^{2+}]_i$. The P2X7R was reported to be present as the P2X7j variant with a weight of approximately 43 kDa in human conjunctival epithelial cells (Guzman-Aranguez et al., 2017). This variant is non-functional, and even suppresses the effects of the normal P2X7Rs (Guzman-Aranguez et al., 2017). Other studies found the functional P2X7 isoform using WB and electrophysiological methods in rat CGCs (McGilligan et al., 2013; Puro, 2020a). Further research is needed to clarify these inconclusive findings. For instance, a YO-PRO-1 experiment investigating pore formation of the P2X7 receptor in response to BzATP treatment could provide useful information about the role of the P2X7R in rat CGCs, perhaps causing cell death (Rat et al., 2017; Virginio et al., 1997).

Our study shows that ATP increases mucin secretion in rat CGCs. The effect of ATP on mucin secretion is supported by other studies that investigated the effect of increasing the $[Ca^{2+}]_i$ on glycoprotein secretion (Bootman and Bultynck, 2020; Dartt et al., 2000; Jumblatt and Jumblatt, 1998). This finding is also in accordance with the response of ATP in goblet cells in other tissues including airways and colon (Petersen

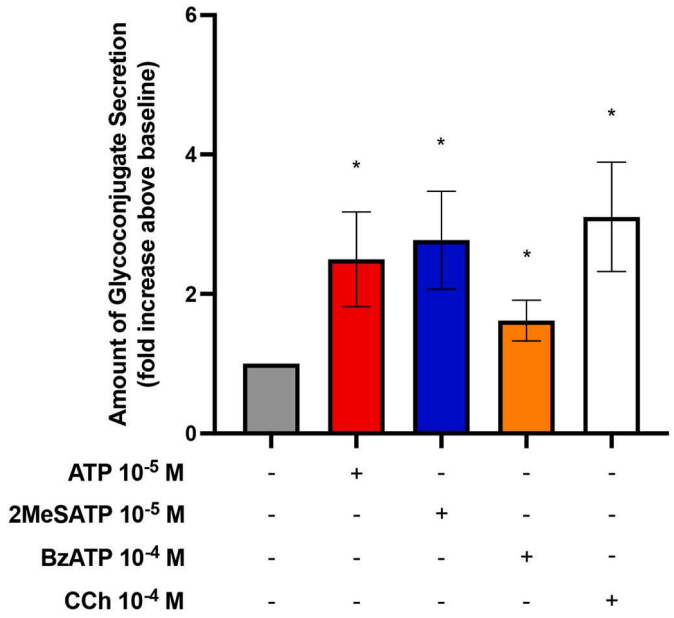

Fig. 7. Effect of 2MeSATP, ATP and BzATP on secretion. Rat conjunctival goblet cells were stimulated with agonists for 2 h before high molecular weight protein secretion measurements. Grey bar: basal, red bar: ATP (10^{-5} M), blue bar: 2MeSATP (10^{-5} M), orange bar: BzATP (10^{-4} M), white bar: CCh (10^{-4} M). Data are mean ± SEM of 9 rats. * indicates significance from basal set to 1.0. (For interpretation of the references to colour in this figure legend, the reader is referred to the Web version of this article.)

and Verkhratsky, 2016; Merlin et al., 1994; Roger et al., 2000). ATP is likely to be released to the ocular surface in several ways to stimulate secretion of protective mucins: 1. from nerve endings together with other neurotransmitters (Lohman et al., 2012; Burnstock et al., 2012), 2. as a result of local cell damage after excessive tear film break-up and increased tear osmolarity, and 3. during acute infections or chronic inflammation resulting in more severe cell damage. Tear film break-up activates corneal and conjunctival sensory nerves (Willcox et al., 2017). This break-up elicits a neural reflex that activates blinking, and mucin secretion through central and peripheral nerves including efferent autonomic nerve fibers and possibly also release of ATP (Dartt and Masli, 2014). Local cell damage may also occur with excessive tear film break-up, which subsequently releases ATP that activates adjacent goblet cells to secrete protective mucins. We previously showed that a priming agent such as toxigenic *S. aureus* is able to activate the NLRP3 inflammasome and increase IL-1β production and that ATP can enhance this process. ATP alone was found to activate caspase 1, but did not induce pro IL-1β synthesis in rat CGCs (McGilligan et al., 2013). This two-step activation process of lL-1β release ensures that ATP can function both as a DAMP-molecule and a mucin inductor during normal conditions. If ATP alone increased mature lL-1β secretion, the normal regulation of mucin production by ATP would be compromised. Furthermore, Panx1 is considered to be activated by caspase-mediated cleavage after inflammasome activation (Sandilos et al., 2012). Therefore, Panx1 activation could further worsen inflammation by causing excessive ATP release. This may result in a vicious circle of inflammation, although restricted by the lack of mature IL-1β production. ATP levels are higher in tears of dry eye disease patients than in control participants (Guzman-Aranguez et al., 2017). One explanation is the prolonged hypertonic and unstable tear film accompanied with this condition, as well as ocular inflammation that can cause ATP release (Willcox et al., 2017; Guzman-Aranguez et al., 2017). In summary, ATP appears to play a dual role on the ocular surface. It can act as a normal regulator of mucin secretion contributing to a healthy ocular surface. On the other hand, ATP may lead to excessive inflammation that both kills pathogens, but also results in goblet cell death and chronic inflammatory conditions.

ATP elicited a peak $[Ca^{2+}]_i$ response higher than that of BzATP and 2MeSATP. It is likely that a portion of this $[Ca^{2+}]_i$ increase can be attributed to action of P2YRs through ATP stimulation of P2Y2 or P2Y4Rs, and perhaps P1 receptors after hydrolysis of ATP to adenosine by ectonucleotidases (Lee et al., 2002). However, multiple studies have used suramin 10^{-5} and 10^{-4} M to block the P2Y2R, which in our study did not reduce ATP-induced peak $[Ca^{2+}]_i$ (Xie et al., 2014; Li et al., 2014). In addition, an increase in $[Ca^{2+}]_i$ could also be caused by conductance of other cations through the plasma membrane ion channels resulting in polarization and activation of other channels and intracellular signaling pathways (Puro, 2018, 2020b). In this study we used 100 μM BzATP to stimulate the P2X7Rs. In fact, this concentration has been shown to activate several P2XRs, P2YRs, and could even be hydrolyzed to activate P1 receptors as well (Illes et al., 2021; Kukley et al., 2004; Jacobson et al., 2009). More research is needed to investigate which receptors are activated during the large ATP- and BzATP-induced $[Ca^{2+}]_i$ increase in CGCs.

There was no clear evidence of other functional homo- or heterotrimeric P2XRs other than the homotrimeric P2X4R. The ATP-elicited peak $[Ca^{2+}]_i$ was not decreased in the presence of suramin and no distinct $[Ca^{2+}]_i$ change was observed with micromolar addition of α,β-MeATP and β,γ-MeATP. Suramin antagonizes all other P2XRs except for the P2X4 and P2X7Rs at micromolar concentrations, and α,β-MeATP and β,γ-MeATP at a high concentration (100 μM; Supplemental Fig. 5) only elicited a small peak $[Ca^{2+}]_i$ in our study (Torres et al., 1999; Syed and Kennedy, 2012; Illes et al., 2021; Clyne et al., 2002; Burnstock, 2007; Palygin et al., 2018). To confirm our findings, future research on P2XRs in CGCs could utilize specific antagonists for the P2X1 and P2X3Rs, knockout animals (available for all P2X subunits) and metal ions which has been shown to modulate several P2XRs (Illes et al., 2021).

5. Conclusion

Even though all P2XRs are present in rat CGCs, activation of only the homomeric P2X4R increases the $[Ca^{2+}]_i$. ATP also likely regulates $[Ca^{2+}]_i$ through other mechanisms than P2XR activation. Activation of P2X4 receptors, along with other receptors, also stimulates CGC mucin secretion. ATP is implicated in both maintaining a healthy ocular surface by stimulating protective mucin secretion, and in disease as a DAMP-molecule in response to acute infection and chronic inflammation.

Declaration of competing interest

Although not considered a conflict of interest, for the sake of transparency: Tor Paaske Utheim is co-founder and co-owner of The Norwegian dry eye clinic, which delivers talks for and/or receives financial support from the following: ABIGO, Alcon, Allergan, AMWO, Bausch&Lomb, European school for advanced studies in ophthalmology, InnZ Medical, Medilens Nordic, Medistim, Novartis, Santen, Specsavers, Shire and Thea Laboratories. He has served on the global scientific advisory board for Novartis and Alcon as well as the European advisory board for Shire. Utheim is the Norwegian Global Ambassador for Tear Film and Ocular Surface Society (TFOS) and a Board Member of the International Ocular Surface Society. The remaining authors have no conflict of interest to declare.

Funding

This research was funded by NFR 271555/F20 grant by the Norwegian Research Council, through The Medical Student Research Program (H.F. and K.F.), and USPHS NIH grant R01EY 019470 (D.A.D).

Author contributions

Conceptualization, H.F. and D.A.D.; investigation, H.F., K.F., M.Y. and J.B.; writing-original draft, H.F.; writing-review and editing, D.A.D. and T.P.U.; funding acquisition, D.A.D. and T.P.U.; supervision, D.A.D. and M.Y.

Data availability

Data will be made available on request.

Acknowledgement

The authors want to thank Robin R. Hodges MS for her contribution to this project. We also thank Maria Naqvi and Morten Magno for their discussions on the topic.

Appendix A. Supplementary data

Supplementary data to this article can be found online at https://doi.org/10.1016/j.exer.2023.109614.

References

Belleannée, C., Da Silva, N., Shum, W.W., Brown, D., Breton, S., 2010. Role of purinergic signaling pathways in V-ATPase recruitment to apical membrane of acidifying epididymal clear cells. Am. J. Physiol. Cell Physiol. 298 (4), C817–C830.
Bernier, L.P., Ase, A.R., Boué-Grabot, E., Séguéla, P., 2012. P2X4 receptor channels form large noncytolytic pores in resting and activated microglia. Glia 60 (5), 728–737.
Bootman, M.D., Bultynck, G., 2020. Fundamentals of cellular calcium signaling: a primer. Cold Spring Harbor Perspect. Biol. 12 (1).
Brandao-Burch, A., Key, M.L., Patel, J.J., Arnett, T.R., Orriss, I.R., 2012. The P2X7 receptor is an important regulator of extracellular ATP levels. Front. Endocrinol. 3, 41.
Bron, A.J., Tiffany, J.M., Gouveia, S.M., Yokoi, N., Voon, L.W., 2004. Functional aspects of the tear film lipid layer. Exp. Eye Res. 78 (3), 347–360.
Burnstock, G., 2007. Purine and pyrimidine receptors. Cell. Mol. Life Sci. 64 (12), 1471–1483.
Burnstock, G., Brouns, I., Adriaensen, D., Timmermans, J.P., 2012. Purinergic signaling in the airways. Pharmacol. Rev. 64 (4), 834–868.
Buvinic, S., Almarza, G., Bustamante, M., Casas, M., López, J., Riquelme, M., et al., 2009. ATP released by electrical stimuli elicits calcium transients and gene expression in skeletal muscle. J. Biol. Chem. 284 (50), 34490–34505.
Clyne, J.D., LaPointe, L.D., Hume, R.I., 2002. The role of histidine residues in modulation of the rat P2X(2) purinoceptor by zinc and pH. J. Physiol. 539 (Pt 2), 347–359.
Dartt, D.A., Masli, S., 2014. Conjunctival epithelial and goblet cell function in chronic inflammation and ocular allergic inflammation. Curr. Opin. Allergy Clin. Immunol. 14 (5), 464–470.
Dartt, D.A., Willcox, M.D., 2013. Complexity of the tear film: importance in homeostasis and dysfunction during disease. Exp. Eye Res. 117, 1–3.
Dartt, D.A., Rios, J.D., Kanno, H., Rawe, I.M., Zieske, J.D., Ralda, N., et al., 2000. Regulation of conjunctival goblet cell secretion by Ca(2+)and protein kinase C. Exp. Eye Res. 71 (6), 619–628.
Diezmos, E.F., Bertrand, P.P., Liu, L., 2016. Purinergic signaling in gut inflammation: the role of connexins and pannexins. Front. Neurosci. 10, 311.
Diezmos, E.F., Markus, I., Perera, D.S., Gan, S., Zhang, L., Sandow, S.L., et al., 2018. Blockade of pannexin-1 channels and purinergic P2X7 receptors shows protective effects against cytokines-induced colitis of human colonic mucosa. Front. Pharmacol. 9, 865.
Donnelly-Roberts, D.L., Namovic, M.T., Han, P., Jarvis, M.F., 2009. Mammalian P2X7 receptor pharmacology: comparison of recombinant mouse, rat and human P2X7 receptors. Br. J. Pharmacol. 157 (7), 1203–1214.
Gipson, I.K., Argüeso, P., 2003. Role of mucins in the function of the corneal and conjunctival epithelia. Int. Rev. Cytol. 231, 1–49.
Guzman-Aranguez, A., Pérez de Lara, M.J., Pintor, J., 2017. Hyperosmotic stress induces ATP release and changes in P2X7 receptor levels in human corneal and conjunctival epithelial cells. Purinergic Signal. 13 (2), 249–258.
Hodges, R.R., Dartt, D.A., 2013. Tear film mucins: front line defenders of the ocular surface; comparison with airway and gastrointestinal tract mucins. Exp. Eye Res. 117, 62–78.
Hodges, R.R., Vrouvlianis, J., Scott, R., Dartt, D.A., 2011. Identification of $P2X_3$ and $P2X_7$ purinergic receptors activated by ATP in rat lacrimal gland. Invest. Ophthalmol. Vis. Sci. 52 (6), 3254–3263.
Illes, P., Müller, C.E., Jacobson, K.A., Grutter, T., Nicke, A., Fountain, S.J., et al., 2021. Update of P2X receptor properties and their pharmacology: IUPHAR Review 30. Br. J. Pharmacol. 178 (3), 489–514.
Jacobson, K.A., Ivanov, A.A., de Castro, S., Harden, T.K., Ko, H., 2009. Development of selective agonists and antagonists of P2Y receptors. Purinergic Signal. 5 (1), 75–89.
Jumblatt, J.E., Jumblatt, M.M., 1998. Regulation of ocular mucin secretion by P2Y2 nucleotide receptors in rabbit and human conjunctiva. Exp. Eye Res. 67 (3), 341–346.
Kanellopoulos, J.M., Almeida-da-Silva, C.L.C., Rüütel Boudinot, S., Ojcius, D.M., 2021. Structural and functional features of the P2X4 receptor: an immunological perspective. Front. Immunol. 12, 645834.
Kukley, M., Stausberg, P., Adelmann, G., Chessell, I.P., Dietrich, D., 2004. Ecto-nucleotidases and nucleoside transporters mediate activation of adenosine receptors on hippocampal mossy fibers by P2X7 receptor agonist 2'-3'-O-(4-benzoylbenzoyl)-ATP. J. Neurosci. 24 (32), 7128–7139.
Lai, C.P., Bechberger, J.F., Thompson, R.J., MacVicar, B.A., Bruzzone, R., Naus, C.C., 2007. Tumor-suppressive effects of pannexin 1 in C6 glioma cells. Cancer Res. 67 (4), 1545–1554.
Lazarowski, E.R., Boucher, R.C., 2009. Purinergic receptors in airway epithelia. Curr. Opin. Pharmacol. 9 (3), 262–267.
Lee, V.H.L., Kulkarni, A.A., Shiue, M.H.I., 2002. Nucleoside and nucleotide stimulation of fluid secretion in the pigmented rabbit conjunctiva. In: Sullivan, D.A., Stern, M.E., Tsubota, K., Dartt, D.A., Sullivan, R.M., Bromberg, B.B. (Eds.), Lacrimal Gland, Tear Film, and Dry Eye Syndromes 3: Basic Science and Clinical Relevance Part A and B. Springer US, Boston, MA, pp. 249–254.
Li, D., Carozza, R.B., Shatos, M.A., Hodges, R.R., Dartt, D.A., 2012. Effect of histamine on Ca(2+)-dependent signaling pathways in rat conjunctival goblet cells. Invest. Ophthalmol. Vis. Sci. 53 (11), 6928–6938.
Li, N., Lu, Z.Y., Yu, L.H., Burnstock, G., Deng, X.M., Ma, B., 2014. Inhibition of G protein-coupled P2Y2 receptor induced analgesia in a rat model of trigeminal neuropathic pain. Mol. Pain 10, 21.
Lohman, A.W., Billaud, M., Isakson, B.E., 2012. Mechanisms of ATP release and signalling in the blood vessel wall. Cardiovasc. Res. 95 (3), 269–280.
McGilligan, V.E., Gregory-Ksander, M.S., Li, D., Moore, J.E., Hodges, R.R., Gilmore, M.S., et al., 2013. Staphylococcus aureus activates the NLRP3 inflammasome in human and rat conjunctival goblet cells. PLoS One 8 (9), e74010.
Merlin, D., Augeron, C., Tien, X.Y., Guo, X., Laboisse, C.L., Hopfer, U., 1994. ATP-stimulated electrolyte and mucin secretion in the human intestinal goblet cell line HT29-Cl.16E. J. Membr. Biol. 137 (2), 137–149.
Nicke A, Grutter T, Egan TM. P2X Receptors. [cited 8/23/2022]. In: The Oxford Handbook of Neuronal Ion Channels [Internet]. Oxford University Press, [cited 8/23/2022]; [0]. Available from: https://doi.org/10.1093/oxfordhb/9780190669164.013.7.
North, R.A., 2002. Molecular physiology of P2X receptors. Physiol. Rev. 82 (4), 1013–1067.
Palygin, O., Ilatovskaya, D.V., Levchenko, V., Klemens, C.A., Dissanayake, L., Williams, A.M., et al., 2018. Characterization of purinergic receptor expression in ARPKD cystic epithelia. Purinergic Signal. 14 (4), 485–497.
Paredes-Gamero, E.J., França, J.P., Moraes, A.A., Aguilar, M.O., Oshiro, M.E., Ferreira, A.T., 2004. Problems caused by high concentration of ATP on activation of the P2X7 receptor in bone marrow cells loaded with the Ca2+ fluorophore fura-2. J. Fluoresc. 14 (6), 711–722.
Petersen, O.H., Verkhratsky, A., 2016. Calcium and ATP control multiple vital functions. Philos. Trans. R. Soc. Lond. B Biol. Sci. 371 (1700).
Prasad, M., Fearon, I.M., Zhang, M., Laing, M., Vollmer, C., Nurse, C.A., 2001. Expression of P2X2 and P2X3 receptor subunits in rat carotid body afferent neurones: role in chemosensory signalling. J. Physiol. 537 (Pt 3), 667–677.
Puro, D.G., 2018. Role of ion channels in the functional response of conjunctival goblet cells to dry eye. Am. J. Physiol. Cell Physiol. 315 (2), C236-c46.
Puro, D.G., 2020a. How goblet cells respond to dry eye: adaptive and pathological roles of voltage-gated calcium channels and P2X(7) purinoceptors. Am. J. Physiol. Cell Physiol. 318 (6), C1305-c15.
Puro, D.G., 2020b. Bioelectric responses of conjunctival goblet cells to dry eye: impact of ion channels on exocytotic function and viability. Int. J. Mol. Sci. 21 (24).
Rat, P., Olivier, E., Tanter, C., Wakx, A., Dutot, M., 2017. A fast and reproducible cell- and 96-well plate-based method for the evaluation of P2X7 receptor activation using YO-PRO-1 fluorescent dye. J Biol Methods 4 (1), e64.
Roger, P., Gascard, J.P., Bara, J., de Montpreville, V.T., Yeadon, M., Brink, C., 2000. ATP induced MUC5AC release from human airways in vitro. Mediat. Inflamm. 9 (6), 277–284.
Samways, D.S., Li, Z., Egan, T.M., 2014. Principles and properties of ion flow in P2X receptors. Front. Cell. Neurosci. 8, 6.
Sandilos, J.K., Chiu, Y.H., Chekeni, F.B., Armstrong, A.J., Walk, S.F., Ravichandran, K.S., et al., 2012. Pannexin 1, an ATP release channel, is activated by caspase cleavage of its pore-associated C-terminal autoinhibitory region. J. Biol. Chem. 287 (14), 11303–11311.
Seol, D., Choe, H., Zheng, H., Jang, K., Ramakrishnan, P.S., Lim, T.H., et al., 2011. Selection of reference genes for normalization of quantitative real-time PCR in organ culture of the rat and rabbit intervertebral disc. BMC Res. Notes 4, 162.
Shatos, M.A., Ríos, J.D., Horikawa, Y., Hodges, R.R., Chang, E.L., Bernardino, C.R., et al., 2003. Isolation and characterization of cultured human conjunctival goblet cells. Invest. Ophthalmol. Vis. Sci. 44 (6), 2477–2486.
Stokes, L., Layhadi, J.A., Bibic, L., Dhuna, K., Fountain, S.J., 2017. P2X4 receptor function in the nervous system and current breakthroughs in pharmacology. Front. Pharmacol. 8, 291.
Syed, N-i-H, Kennedy, C., 2012. Pharmacology of P2X receptors. Wiley Interdiscip. Rev.: Membrane Transport and Signaling 1 (1), 16–30.
The definition and classification of dry eye disease: report of the definition and classification subcommittee of the international dry eye WorkShop. Ocul. Surf. 5 (2), 2007, 75–92, 2007.

Torres, G.E., Egan, T.M., Voigt, M.M., 1999. Hetero-oligomeric assembly of P2X receptor subunits. Specificities exist with regard to possible partners. J. Biol. Chem. 274 (10), 6653–6659.

Virginio, C., Church, D., North, R.A., Surprenant, A., 1997. Effects of divalent cations, protons and calmidazolium at the rat P2X7 receptor. Neuropharmacology 36 (9), 1285–1294.

Willcox, M.D.P., Argüeso, P., Georgiev, G.A., Holopainen, J.M., Laurie, G.W., Millar, T.J., et al., 2017. TFOS DEWS II tear film report. Ocul. Surf. 15 (3), 366–403.

Winkelmann, V.E., Thompson, K.E., Neuland, K., Jaramillo, A.M., Fois, G., Schmidt, H., et al., 2019. Inflammation-induced upregulation of P2X(4) expression augments mucin secretion in airway epithelia. Am. J. Physiol. Lung Cell Mol. Physiol. 316 (1), L58–l70.

Xie, R., Xu, J., Wen, G., Jin, H., Liu, X., Yang, Y., et al., 2014. The P2Y2 nucleotide receptor mediates the proliferation and migration of human hepatocellular carcinoma cells induced by ATP. J. Biol. Chem. 289 (27), 19137–19149.

Yang, Y., Delalio, L.J., Best, A.K., Macal, E., Milstein, J., Donnelly, I., et al., 2020a. Endothelial pannexin 1 channels control inflammation by regulating intracellular calcium. J. Immunol. 204 (11), 2995–3007.

Yang, M., Lippestad, M., Hodges, R.R., Fjærvoll, H.K., Fjærvoll, K.A., Bair, J.A., et al., 2020b. RvE1 uses the LTB(4) receptor BLT1 to increase [Ca(2+)](i) and stimulate mucin secretion in cultured rat and human conjunctival goblet cells. Ocul. Surf. 18 (3), 470–482.

Zhang, Y., Sanchez, D., Gorelik, J., Klenerman, D., Lab, M., Edwards, C., et al., 2007. Basolateral P2X4-like receptors regulate the extracellular ATP-stimulated epithelial Na+ channel activity in renal epithelia. Am. J. Physiol. Ren. Physiol. 292 (6), F1734–F1740.